THE ASTROPHYSICAL JOURNAL, 653: L81–L84, 2006 December 20

TEMPORAL PROFILES AND SPECTRAL LAGS OF XRF 060218

EN-WEI LIANG,[1,2] BIN-BIN ZHANG,[1,3,4] MIKE STAMATIKOS,[5] BING ZHANG,[1] JAY NORRIS,[5] NEIL GEHRELS,[5] JIN ZHANG,[3,4] AND Z. G. DAI[1,6]

Received 2006 June 18; accepted 2006 October 31; published 2006 December 6

ABSTRACT

The spectral and temporal properties of the nonthermal emission of the nearby XRF 060218 in the 0.3–150 keV band are studied. We show that both the spectral energy distribution and the light-curve properties suggest the same origin of the nonthermal emission detected by *Swift* BAT and XRT. This event has the longest pulse duration and spectral lag observed to date among the known GRBs. The pulse structure and its energy dependence are analogous to typical GRBs. By extrapolating the observed spectral lag to the *Compton Gamma Ray Observatory* (*CGRO*) BATSE bands we find that the hypothesis that this event complies with the same luminosity-lag relation with bright GRBs cannot be ruled out at 2 σ significance level. These intriguing facts, along with its compliance with the Amati relation, indicate that XRF 060218 shares the similar radiation physics as typical GRBs.

Subject headings: gamma rays: bursts — methods: statistical

Online material: color figures

1. INTRODUCTION

X-ray flashes (XRFs), cosmic explosions with lower spectral peak energies (E_p) in νF_ν spectra than typical gamma-ray bursts (GRBs; Heise et al. 2001; Kippen et al. 2003), are thought to be the low-energy extension of typical GRBs (Lamb et al. 2005; Sakamoto et al. 2004, 2006; Cui et al. 2005). They may be GRB jets (uniform or structured) viewed at off-axis directions (e.g., Zhang et al. 2003, 2004; Yamazaki et al. 2004) or intrinsically different events (Lamb et al. 2005; Soderberg et al. 2005). It is long speculated that long-duration GRBs originate from a relativistic jet emerging from a collapsing massive star progenitor (Woosley et al. 1993; Paczynski 1998; MacFadyen & Woosley 1999; Zhang et al. 2003), and associations of core-collapsing supernovae (SNe) with long GRB afterglows have been spectroscopically identified in a number of systems, including GRB 980425/SN 1998bw (Galama et al. 1998), GRB 030329/SN2003 dhr (Stanek et al. 2003; Hjorth et al. 2003), and GRB 031203/SN 2003lw (Malesani et al. 2004). The firm spectroscopic association of the nearby XRF 060218 (at $z = 0.0331$; Mirabal et al. 2006) detected by *Swift* (Campana et al. 2006) with the Type Ic SN 2006aj was established recently (Modjaz et al. 2006; Pian et al. 2006; Sollerman et al. 2006; Mirabal et al. 2006; Cobb et al. 2006; Soderberg et al. 2006). This suggests that the progenitors of both GRBs and XRFs are related to the death of massive stars, and XRFs are the low-energy extension of the more "standard" GRBs.

Some empirical relations have been discovered from typical GRBs. It is interesting to verify whether XRF 060218 satisfies these relations as an approach to access its "standardness." It has been reported that XRF 060218 complies with the isotropic energy versus the spectral peak energy ($E_{\rm iso}$-E_p) relation derived from long GRBs (Amati et al. 2002) and other XRFs (Amati et al. 2006). The pulses in GRB light curves usually display a fast-rise-exponential-decay (FRED) shape, and the pulse width is related to the energy of the observational band as $\omega \propto E^{-0.4}$ (Fenimore et al. 1995; Norris et al. 2005). A correlation between the isotropic luminosity and the spectral lag ($L_{\rm iso}$-τ relation) of light curves was also discovered with typical GRBs as $L_{\rm iso} \propto \tau^{-1.18}$ (Norris et al. 2000). Both ω-E and $L_{\rm iso}$-τ relations are related to the light curves. Since most photons of an XRF are in the X-ray band, previous GRB missions did not observe the real light curves of XRFs. XRF 060218 is long and soft, and *Swift* Burst Alert Telescope (BAT) and X-Ray Telescope (XRT) simultaneously collected the data in the gamma-ray to X-ray bands. This makes it possible to measure its temporal structure and to examine whether it complies with the same ω-E and $L_{\rm iso}$-τ relations derived from GRBs. In this Letter we focus on this issue. Throughout the Letter $H_0 = 71$ km s^{-1} Mpc^{-1}, $\Omega_m = 0.3$, and $\Omega_\Lambda = 0.7$ are adopted.

2. DATA

XRF 060218 was detected with the *Swift* BAT on 2006 February 18.149 UT. Its duration $T_{90} \sim 2000$ s in the 15–150 keV band. *Swift* slewed autonomously to the burst, and the XRT and UV/Optical Telescope began collecting data 159 s after the burst trigger.

XRF 060218 was an image trigger. The BAT event data lasted only until $t \sim 300$ s after the trigger. The survey data are used to derive the BAT light curve. XRF 060218 is very soft, with most of the emission in the BAT band being lower than 50 keV (Campana et al. 2006). In order to obtain a high level of signal-to-noise ratio of the BAT light curve, we use the light curve in the whole BAT band, i.e., 15–150 keV. The first orbit of the XRT data is fully in the Windowed Timing mode. We extract the light curves and spectrum of the XRT data with the Xselect package. The spectrum is grouped with the tool `grppha`, and the spectral fitting is carried out with the Xspec package. Following Campana et al. (2006) we fit the XRT spectrum in the first orbit with a model combining a blackbody component with temperature kT and a cutoff power law ($F \propto E^{-\Gamma} e^{-E/E_c}$) component. The absorption in both the Milky Way ($N_{\rm H} \sim 1.1$ cm^{-2}; Dickey & Lockman 1990) and the GRB host galaxy ($N_{\rm H}^{\rm host}$) is incorporated. We obtain $N_{\rm H}^{\rm host} = 0.63^{+0.03}_{-0.03} \times 10^{22}$ cm^{-2}, $kT = 0.122^{+0.003}_{-0.004}$ keV, $\Gamma = 1.78^{+0.08}_{-0.08}$, and $E_c = 21.8^{+15.8}_{-6.7}$ keV (corre-

[1] Department of Physics, University of Nevada, Las Vegas, NV 89154; lew@physics.unlv.edu, bzhang@physics.unlv.edu.
[2] Department of Physics, Guangxi University, Nanning 530004, China.
[3] National Astronomical Observatories/Yunnan Observatory, Chinese Academy of Sciences, Kunming 650011, China.
[4] Graduate School of the Chinese Academy of Sciences, Beijing 100039, China.
[5] NASA Goddard Space Flight Center, Greenbelt, MD 20771.
[6] Department of Astronomy, Nanjing University, Nanjing 210093, China.

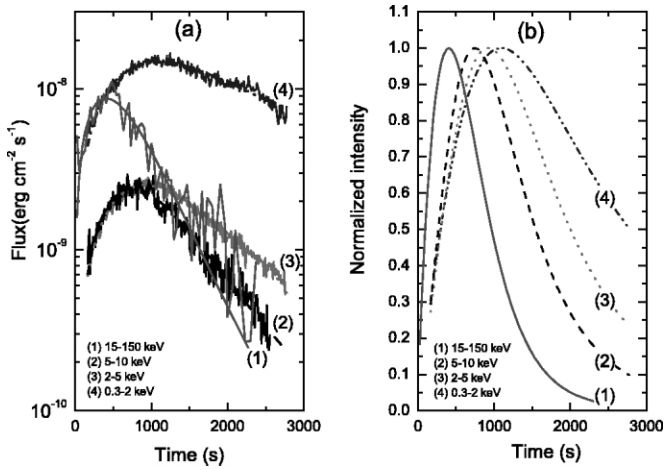

FIG. 1.—(*a*) Unabsorbed light curves of the nonthermal gamma rays/X-rays in the energy bands of 15–150, 5–10, 2–5, and 0.3–2 keV, respectively. The fitting curves with eq. (1) are plotted. (*b*) Normalized light curves from the empirical model fitting. [*See the electronic edition of the Journal for a color version of this figure.*]

sponding to $E_p \sim 5$ keV), with reduced $\chi^2 = 1.55$ for 769 degrees of freedom. We derive the unabsorbed light curves in the 0.3–2, 2–5, and 5–10 keV bands and subtract the thermal component with the parameters reported by Campana et al. (2006), since it is likely of different origin (e.g., the shock breakout emission associated with SN 2006aj [Campana et al. 2006]; cf. Li 2006; Ghisellini et al. 2006b). We therefore subtract the contribution of this component from the observed light curves. The kT and the radiation radii ($R_{\rm BB}$) evolve with time during the first orbit. We read the values of kT and $R_{\rm BB}$ from Campana et al. (2006) and calculate the light curves of this component in 0.3–2, 2–5, and 5–10 keV bands. Since the temperature of the blackbody component is below 0.2 keV, the light curves in the energy band higher than 2 keV is essentially not contaminated by the thermal component. In the 0.3–2 keV band, the derived light curve of the thermal component continuously increase with time, which could be well fitted by $\log F_{0.3-2} = (-10.69 \pm 0.09) + (0.66 \pm 0.03) \log t$ in cgs units. We thus subtract the contribution of this component from the 0.3–2 keV band light curve according to this fitting result. The derived nonthermal light curves in the three XRT bands as well as the one in the BAT band are shown in Figure 1*a*. To clearly view the pulse width and spectral lag dependences with energy, we also plot in Figure 1*b* the normalized light curves. The characteristics of the light curves along with the average photon energy (E) of each energy band are reported in Tables 1 and 2.

3. RESULTS

3.1. *Spectral Energy Distribution*

One important question is whether the XRT nonthermal emission and the BAT emission are of the same origin. In order to clarify this, we first study the spectral energy distribution (SED) of the burst using joint BAT-XRT data. Since this event is image trigger, the BAT event file contains only the data in the first 300 s since the BAT trigger. XRT began collecting data 159 s after the BAT trigger. We thus only obtain simultaneous observations of the two instruments from 160 to 300 s with the event files. The joint-fit SED in this period is shown in Figure 2, which is well fitted by the BB+CPL model (Campana et al. 2006) with the following parameters: $N_{\rm H}^{\rm host} = 0.65^{+0.03}_{-0.03} \times 10^{22}$ cm^{-2}, $kT = 0.13^{+0.01}_{-0.01}$ keV, $\Gamma = 1.56^{+0.08}_{-0.07}$, and $E_c = 122^{+160}_{-46}$ keV (corresponding to $E_p \sim 54$ keV), with reduced $\chi^2 = 0.97$ for 327 degrees of freedom. The E_p strongly evolves with time, from 54 keV at the beginning down to ~5 keV at later times. This is consistent with that reported by Campana et al. (2006) and Ghisellini et al. (2006a). The model fitting results are shown in Figure 2. One can observe that the BAT component is a good extrapolation of the XRT nonthermal component. This result implies that the nonthermal emissions detected by XRT and BAT are of the same origin.

TABLE 1
TEMPORAL STRUCTURES OF THE LIGHT CURVES

Band (keV)	Peak (s)	ω (s)	φ	$\bar{E}$ (keV)
(1) 15–150	405(25)	889(244)	0.54(0.18)	36.9
(2) 5–10	735(9)	1278 (45)	0.59(0.03)	6.9
(3) 2–5	919(7)	1707(40)	0.58(0.02)	3.1
(4) 0.3–2	1082(13)	2625(125)	0.43(0.03)	0.7

TABLE 2
SPECTRAL LAGS OF THE LIGHT CURVES

Bands	ΔE (keV)	$\tau_{\rm peak}$ (s)	$\tau_{\rm CCF}$ (s)	Bands	ΔE (keV)	$\tau_{\rm peak}$ (s)
(1)–(2)	30	330(26)	249(37)	(1)–(3)	33.8	514(26)
(1)–(4)	36.2	677(28)	518(70)	(2)–(3)	3.8	184(11)
(2)–(4)	6.19	347(16)	173(25)	(3)–(4)	2.4	163(15)

3.2. *Pulse Width and Energy Dependence*

As shown in Figure 1, the light curves in different energy bands can all be modeled by a single FRED pulse. Kocevski et al. (2003) developed an empirical expression to fit a FRED-like pulse, which reads

$$F(t) = F_m \left(\frac{t + t_0}{t_m + t_0}\right)^r \left[\frac{d}{d + r} + \frac{r}{d + r}\left(\frac{t + t_0}{t_m + t_0}\right)^{(r+1)}\right]^{-[(r+d)/(r+1)]}, \quad (1)$$

where t_m is the time of the maximum flux (F_m), t_0 is the offset time, and r and d are the rising and decaying power-law indices, respectively. We fit the light curves with equation (1) and then measure the pulse width, rising and decaying times at the FWHM of the fitting light curves, and the rising-to-decaying

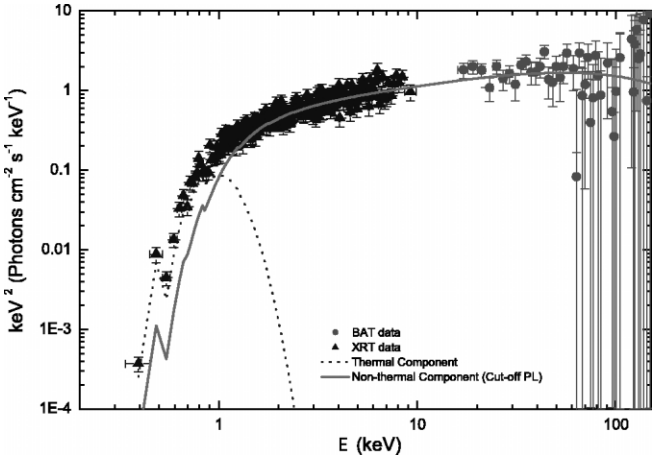

FIG. 2.—BAT-XRT joint spectral energy distribution from 160 to 300 s since the BAT trigger. The BB+CutoffPL fitting model is also shown. [*See the electronic edition of the Journal for a color version of this figure.*]

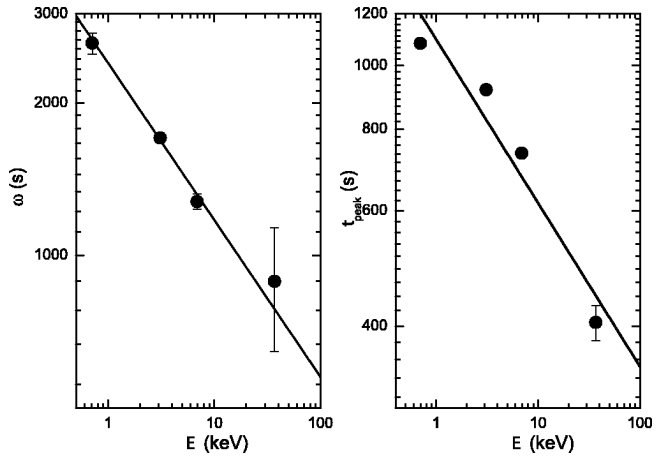

FIG. 3.—Pulse duration (*left*) and the peak time (*right*) as a function of the average photon energy of the nonthermal emission. The solid lines in both panels are the best fits.

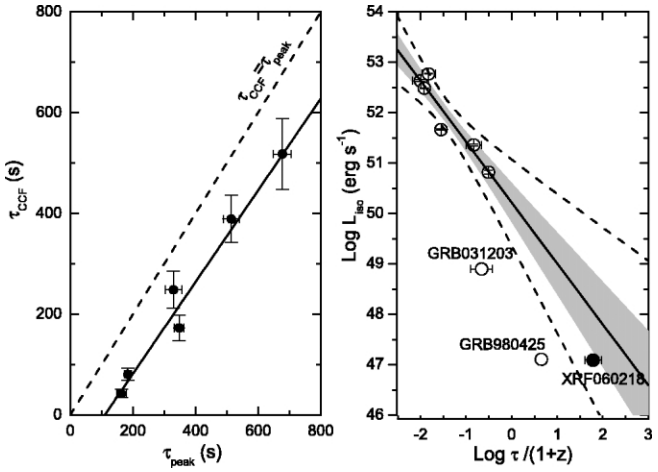

FIG. 4.—*Left*: Comparison of the spectral lags derived from the peak times and from the CCF method. The solid line is the best fit. *Right*: Isotropic gamma-ray luminosity as a function of spectral lag. The spectral lags of typical GRBs and GRB 980425 are calculated with the light curves in the 25–50 and 100–300 keV bands observed by *CGRO* BATSE. The lag of GRB 031203 is calculated with the light curves in the 20–50 and 100–200 keV bands. The gray band and the two dashed lines mark the best fits at the 1 and 2 σ confidence level, respectively, and the solid line is the regression line for the six typical GRBs presented in Norris et al. (2000).

time ratio (φ). The errors of these quantities are derived from simulations by assuming a normal distribution of the errors of the fitting parameters. The reported errors are at 1 σ confidence level. The results are tabulated in Table 1. We show ω as a function of E in Figure 3 (*left*). Apparently the two quantities are correlated. A best fit yields $\omega \propto E^{-0.31\pm0.03}$. The φ parameter ranges from 0.43 to 0.59. It is found that XRF 060218 roughly satisfies the same ω-E relation (Fenimore et al. 1995; Norris et al. 2005), and its φ values are also well consistent with that observed in typical GRBs (e.g., Norris et al. 1996; Liang et al. 2002), although it has a much longer pulse width than other single-pulse GRBs. These results imply that XRF 060218 may be an extension of GRBs to the extremely long and soft regime.

3.3. *Spectral Lag and Energy Dependence*

The light curves shown in Figure 1*a* display a significant spectral lag (τ), with soft photons lagging behind the hard photons, as usually seen in long GRBs (Norris et al. 2000; Yi et al. 2006). We illustrate this lag behavior with the intensity-normalized light curves in Figure 1*b*. The light curves peak at 405 ± 25, 735 ± 9, 919 ± 7, and 1082 ± 13 s, respectively, in a sequence of high-energy band to low-energy band as shown in Figure 3 (*right*). The best fit to the correlation between the peak time ($t_{\rm peak}$) and the average photon energy yields

$$\log t_{\rm peak} = (3.04 \pm 0.04) - (0.25 \pm 0.05) \log E. \quad (2)$$

A simple estimate of the lags between any pairs of the four light curves obtains $\tau_{\rm peak} = 163 \sim 677$ s, being consistent with that shown in Gehrels et al. (2007). We note XRF 060218 becomes the new record holder of the long-lag, wide-pulse GRBs. The previous record holder was GRB 971208, with $\tau \sim 58$ s and $\omega = 395$ s (Norris et al. 2005).

We also calculate the lags with the cross-correlation function (CCF) method. The errors of lags are evaluated by simulations. The results are also reported in Table 2. The lag derived by the CCF method ($\tau_{\rm CCF}$) is strongly correlated with $\tau_{\rm peak}$ but is systematically lower[7] than $\tau_{\rm peak}$ (Fig. 4 [*left*]). A best fit gives $\tau_{\rm CCF} = (-100 \pm 17) + (0.91 \pm 0.08)\tau_{\rm peak}$.

The $L_{\rm iso}$-τ relation was discovered with six bright BATSE GRBs (Norris et al. 2000), and the spectral lag was defined by the light curves in the 25–50 and 100–300 keV bands. We investigate whether the lag behavior of XRF 060218 is consistent with the $L_{\rm iso}$-τ relation. Since XRF 060218 is a soft XRF and the emission in the 100–300 keV band is too weak to derive a light curve, we assume that $t_{\rm peak}$ of the light curve in the 100–300 keV band follows the $t_{\rm peak}$-E relation (eq. [2]) and perform the extrapolation. With the extrapolated $t_{\rm peak}$ we then estimate $\tau_{\rm peak}$ for the light curves in the 25–50 keV (average energy 30 keV) and 100–300 keV (average energy 200 keV) bands. We obtain $\tau_{\rm peak} = 177 \pm 16$ s. Since $\tau_{\rm CCF}$ is more reliable, we use the $\tau_{\rm peak}$-$\tau_{\rm CCF}$ relation (Fig. 4 [*left*]) to derive $\tau_{\rm CCF} = 61 \pm 26$ s. This lag is used in the L-τ relation analysis. Using the peak fluxes in the BAT and XRT band, we estimate $L_{\rm iso} = 1.2 \times 10^{47}$ ergs s^{-1}.

Figure 4 (*right*) shows the $L_{\rm iso}$-τ relation derived by Norris et al. (2000) compared against XRF 060218 as well as two other nearby GRBs, 980425 and 031203. The data of the previous GRBs are taken from Norris et al. (2000) and Sazonov et al. (2004).[8] The gray band and the two dashed lines mark the best fits at the 1 and 2 σ confidence level, respectively, and the solid line is the regression line for the six GRBs that were used to draw the L-τ correlation; i.e., $\log L_{\rm iso} = (50.22 \pm 0.32) - (1.21 \pm 0.21) \log \tau$ (errors are at the 1 σ level). We can see that XRF 060218 is definitely inside the 2 σ region and is marginally

[7] We here derive $\tau_{\rm CCF}$ from the peak of the CCF without considering the side lobe contribution of the CCF. A fit to the CCF with a cube or quartic function gives a larger lag by considering the side lobe contribution (Norris et al. 2000). However, this method strongly depends on the artificially selected range of CCF for the fitting. Since the light curves are a smooth pulse and their lags are significantly larger than the time bin, the peaks of CCFs are robust to estimate the lags.

[8] The peak photon fluxed in the 50–300 keV bands of these GRBs are converted to energy fluxes with the spectral index presented in Friedman & Bloom (2005), and their $L_{\rm iso}$-values are recalculated with the cosmological parameters used in this Letter.

at the 1 σ region boundary. Therefore, the hypothesis that XRF 060218 follows the L-τ relation cannot be ruled out at the 2 σ significance level. We caution that the τ is inferred from the extrapolation of the $t_{\rm peak}$-E relation. This introduces uncertainties in deriving the lag. The other two nearby GRBs, 980425 and 031203, are out of the 2 σ region, which are identified as significant outliers of this relation (e.g., Sazonov et al. 2004).

4. DISCUSSION AND CONCLUSIONS

We have investigated the nonthermal emission of XRF 060218. The early SED of this event from 0.3–150 keV observed by BAT and XRT suggests that the nonthermal emission detected by the two instruments are the same component. By subtracting the contribution of the thermal emission we derive the light curves of the nonthermal emission. They are composed of a broad single pulse, and the energy dependences of the widths and the rising-to-decaying-time ratio of the pulses are roughly consistent with those derived in typical GRBs. The light curves show significant spectral lags, with a well-defined peak time sequence from high-energy band to low-energy bands; i.e., $t_{\rm peak} \propto E^{-0.25\pm0.05}$. We infer the spectral lag in the BATSE bands and find that the hypothesis that this event complies with the $L_{\rm iso}$-τ relation with typical GRBs cannot be ruled out at the 2 σ significance level.

These intriguing facts, along with its compliance with the Amati relation, strongly suggest that GRB 060218 is a standard burst at the very faint, long, and soft end of the GRB distribution. Since all these relations concern the temporal and spectral properties of emission, they are likely related to the radiation mechanisms. The results therefore imply that XRF 060218 and other XRFs may share the similar radiation physics (e.g., synchrotron or inverse Compton scattering in internal shocks; Mészáros 2002, 2006; Zhang & Mészáros 2004; Piran 2005) with harder GRBs.

As discovered by Norris (2002) with the BATSE GRB sample, long-lag bursts tend to be underluminous. Taken together with the fact that three nearby GRBs, 980425, 031203, and 060218, are long-lagged and underluminous, an intuitive speculation is that long-lag bursts are probably relatively nearby (e.g., Norris et al. 2005). The local GRB rate of these GRBs should thus be much higher than that expected from the high-luminosity GRBs (Liang et al. 2006; see also Cobb et al. 2006; Pian et al. 2006; Soderberg et al. 2006). A possible scenario to explain their wide-pulse, long-lag, and underluminous features is the off-axis viewing angle effect (e.g., Nakamura 1999; Salmonson 2000; Ioka & Nakamura 2001). Another scenario is that these features are intrinsic, being due to their lower Lorentz factors (Kulkarni et al. 1998; Woosley & MacFadyen 1999; Salmonson 2000; Dai et al. 2006; Wang et al. 2006). They might be from a unique GRB population (Liang et al. 2006), having a different type of central engine (e.g., neutron stars rather than black holes) from bright GRBs (e.g., Mazzali et al. 2006; Soderberg et al. 2006; Toma et al. 2006).

We thank the anonymous referee for helpful suggestions, and S. Campana, D. Burrows, J. Nousek, K. Page, T. Sakamoto, X.-Y. Wang, and Z. Li for discussion. This work was supported by NASA under grants NNG06GH62G and NNG05GB67G, and the National Natural Science Foundation of China under grants 10463001(EWL).

REFERENCES

Amati, L., et al. 2002, A&A, 390, 81
———. 2006, A&A, submitted (astro-ph/0607148)
Campana, S., et al. 2006, Nature, 442, 1008
Cobb, B. E., et al. 2006, ApJ, 645, L113
Cui, X. H., Liang, E. W, & Lu R. J. 2005, Chinese J. Astron. Astrophys., 5, 151
Dai, Z. G, Zhang, B., & Liang, E. W. 2006, preprint (astro-ph/0604510)
Dickey, J. M., & Lockman, F. J. 1990, ARA&A, 28, 215
Fenimore, E. E., et al. 1995, ApJ, 448, L101
Friedman, A. S., & Bloom, J. S. 2005, ApJ, 627, 1
Galama, T. J., et al. 1998, Nature, 395, 670
Gehrels, G., et al. 2007, Nature, in press (astro-ph/0610635)
Ghisellini, G., Ghirlanda, G., Mereghetti, S., Bosnjak, Z., Tavecchio, F., & Firmani, C. 2006a, MNRAS, 372, 1699
Ghisellini, G., Ghirlanda, G., & Tavecchio, F. 2006b, MNRAS, in press (astro-ph/0608555)
Heise, J., et al. 2001, in Gamma-Ray Bursts in the Afterglow Era, ed. E. Costa, F. Frontera, & J. Hjorth (Berlin: Springer), 16
Hjorth, J., et al. 2003, Nature, 423, 847
Ioka, K., & Nakamura, T. 2001, ApJ, 554, L163
Kippen, R. M., et al. 2003, in AIP Conf. Proc. 662, Gamma-Ray Burst and Afterglow Astronomy 2001, ed. G. R. Ricker & R. K. Vanderspek (Melville: AIP), 244
Kocevski, D., Ryde, F., & Liang, E. 2003, ApJ, 596, 389
Kulkarni, S. R., et al. 1998, Nature, 395, 663
Li, L. X. 2006, MNRAS, submitted (astro-ph/0605387)
Liang, E. W., Xie, G. Z., & Su, C. Y. 2002, PASJ, 54, 1
Liang, E. W., Zhang, B., Virgili, F., & Dai, Z. G. 2006, preprint (astro-ph/0605200)
Lamb, D. Q., Donaghy, T. Q., & Graziani, C. 2005, ApJ, 620, 355
MacFadyen, A. I., & Woosley, S. E. 1999, ApJ, 524, 262
Malesani, D., et al. 2004, ApJ, 609, L5
Mazzali, P. A., et al. 2006, Nature, 442, 1018
Mészáros, P. 2002, ARA&A, 40, 137
———. 2006, Rep. Prog. Phys., 69, 2259
Mirabal, N., et al. 2006, ApJ, 643, L99
Modjaz, M., et al. 2006, ApJ, 645, L21
Nakamura, T. 1999, ApJ, 522, L101
Norris, J. P. 2002, ApJ, 579, 386
Norris, J. P., Marani, G. F., & Bonnell, J. T. 2000, ApJ, 534, 248
Norris, J. P., et al. 1996, ApJ, 459, 393
———. 2005, ApJ, 627, 324
Paczýnski, B. 1998, ApJ, 494, L45
Pian, E., et al. 2006, Nature, 442, 1011
Piran, T. 2005, Rev. Mod. Phys., 76, 1143
Sakamoto, T., et al. 2004, ApJ, 602, 875
———. 2006, ApJ, 636, L73
Salmonson, J. D. 2000, ApJ, 544, L115
Sazonov, S. Yu., Lutovinov, A. A., & Sunyaev, R. A. 2004, Nature, 430, 646
Soderberg, A. M., et al. 2005, ApJ, 627, 877
———. 2006, Nature, 442, 1014
Sollerman, J., et al. 2006, A&A, 454, 503
Stanek, K. Z., et al. 2003, ApJ, 591, L17
Toma, K., Ioka, K., Sakamoto, T., & Nakamura, T. 2006, ApJ, submitted (astro-ph/0610867)
Wang, X.-Y., Li, Z., Waxman, E., & Mészáros, P. 2006, ApJ, submitted (astro-ph/0608033)
Woosley, S. E., & MacFadyen, A. I. 1999, A&AS, 138, 499
Woosley, S. E., et al. 1993, ApJ, 405, L273
Yamazaki, R., Ioka, K., & Nakamura, T. 2004, ApJ, 607, L103
Yi, T. F., Liang, E. W., Qin, Y. P., & Lu, R. J. 2006, MNRAS, 367, 1751
Zhang, B., Dai, X., Lloyd-Ronning, N. M., & Mészáros, P. 2004, ApJ, 601, L119
Zhang, B., & Mészáros, P. 2004, Int. J. Mod. Phys. A, 19, 2385
Zhang, W., Woosley, S. E., & MacFadyen, A. I.2003, ApJ, 586, 356